RC77 Gilmore, C., Peters, S., LoVetri, J. and McNeill, M. (2004) *Gpr Target Detection Using a Neural Network Classifier of Image Moments as Invariant Features*, Proceedings of ANTEM'2004/URSI, pp. 83-86, Ottawa, Canada, July 20 - 23.

GPR TARGET DETECTION USING A NEURAL NETWORK CLASSIFIER OF IMAGE MOMENTS AS INVARIANT FEATURES

Colin Gilmore, Scott Peters, Joe LoVetri, Dean McNeill

University of Manitoba, Winnipeg, Canada
cgilmore@ee.umanitoba.ca, speters@ee.umanitoba.ca
lovetri@ee.umanitoba.ca, mcneill@ee.umanitoba.ca

ABSTRACT

Preliminary results of automatically detecting unexploded ordinance (UXO) and landmines using an artificial neural network (ANN) to classify particular features in a ground penetrating radar (GPR) image are given. These features are the so-called invariant moments of a GPR image. The automatic detection algorithm is described and results of experiments conducted for both metal and dielectric targets buried in a sandbox are provided. Currently, only metallic targets can be discriminated by the ANN with many false negative indications occurring.

INTRODUCTION

In the past, GPR techniques have been applied only with limited success to the detection of UXO and landmines. Currently, there are no sufficiently reliable methods for automatically detecting such targets using GPR. It is not expected that GPR, by itself, will successfully deal with the manifold situations in which the UXO/landmine problem can manifest itself, but, given the significance of the problem, it is important to extract the utmost from each applicable technique. We show that, for the restricted set of cases considered herein, an ANN can be use to detect a certain class of UXO and landmines buried in a sandbox.

One advantage of GPR is the large amount of data which can be collected. For example, in the stepped-frequency continuous-wave (SFCW) GPR considered herein, at each monostatic measurement location, the magnitude and phase of the radar response at 501 frequencies inside a chosen bandwidth are recorded. The position of the radar antenna may be moved by as little as one centimetre and a new set of measurements taken. The large amount of information is an advantage for accurate interrogation of the subsurface but efficiently dealing with the information so that automated detection becomes possible is still an issue for research. In order for effective automated target detection and classification to occur, the amount of data must be parsimoniously reduced: reduce the data while maintaining the important features that distinguish a target from a non-target. This process is known as feature extraction. Past attempts at feature extraction have included the use of the continuous and discrete wavelet transform, statistical methods such as moments, resonances and ARMA modelling [1 - 6].

In this research we consider features of a GPR range (or depth) vs. crossrange image which may be used to detect the existence of a target. In GPR terminology, a standard RADAR range profile is called an A-scan while a 2-dimensional image of stacked A-scans, taken at different crossrange locations, is called a B-scan (a 3-dimensional image of stacked B-scans is called a C-scan). In this paper we deal only with A-scans and B-scans. An example of a B-scan is shown in the top portion of Figure 1.

The algorithm used to extract features is called the feature extractor and one of the desirable properties of a feature extractor for GPR is an invariance to certain properties of the GPR image [7]. The extracted features are then used in an ANN classifier. We first briefly describe the construction of B-scans from GPR data and then give the details of the feature extractor algorithm and ANN classifier.

GPR IMAGE FEATURES: INVARIANT MOMENTS

For a feature extractor to be useful in GPR, it must be invariant to several factors [7]. Two of the most important factors are invariance to scale and translational changes because different soils with different permittivities will cause changes in the scale of a range profile and because targets will be buried at varying depths. Thus, if we have a feature extractor operating on a A-scan signal $f(t)$, that results in a feature vector y, that is $FE[f(t)] \Rightarrow y$, then it is desirable to have $FE[f(at)] \Rightarrow y$ and $FE[f(t-\tau)] \Rightarrow y$.

The so-called invariant moments of an image, introduced by Hu [8], have been shown to be invariant to changes in scale, as well as translation and rotation of image features. These moments only apply to two dimensional functions $f(x, y)$. For a discrete image, we start by calculating the central moments as [8, 9]

$$\mu_{pq} = \sum_{v}\sum_{x} (x-\bar{x})^p (y-\bar{y})^q f(x,y)\Delta x \Delta y \,. \qquad (1)$$

The normalized central moments, η_{pq}, are then defined as

$$\eta_{pq} = \frac{\mu_{pq}}{\mu_{00}^{\gamma}} \text{ with } \gamma = \frac{p+q}{2} + 1 \qquad (2)$$

and the set of seven invariant moments are then given by

$$\phi_1 = \eta_{20} + \eta_{02}\,,\ \phi_2 = (\eta_{20} - \eta_{02})^2 + 4\eta_{11}^2 \qquad (3)$$

$$\phi_3 = (\eta_{30} - 3\eta_{12})^2 + (3\eta_{21} - \eta_{03})^2 \qquad (4)$$

$$\phi_4 = (\eta_{30} + \eta_{12})^2 + (\eta_{21} + \eta_{03})^2 \quad (5)$$

$$\begin{aligned}\phi_5 = {} & (\eta_{30} - 3\eta_{12})(\eta_{30} + \eta_{12}) \cdot \\ & [(\eta_{30} + \eta_{12})^2 - 3(\eta_{21} + \eta_{03})^2] + \\ & (3\eta_{21} - \eta_{03})(\eta_{21} + \eta_{03}) \cdot \\ & [3(\eta_{30} + \eta_{12})^2 - (\eta_{21} + \eta_{03})^2]\end{aligned} \quad (6)$$

$$\begin{aligned}\phi_6 = {} & (\eta_{20} - \eta_{02}) \cdot \\ & [(\eta_{30} + \eta_{12})^2 - (\eta_{21} + \eta_{03})^2] + \\ & 4\eta_{11}(\eta_{30} + \eta_{12})(\eta_{21} + \eta_{03})\end{aligned} \quad (7)$$

$$\begin{aligned}\phi_7 = {} & (3\eta_{21} - \eta_{03})(\eta_{30} + \eta_{12}) \cdot \\ & [(\eta_{30} + \eta_{12})^2 - 3(\eta_{21} + \eta_{03})^2] + \\ & (3\eta_{12} - \eta_{30})(\eta_{21} + \eta_{03}) \cdot \\ & [3(\eta_{30} + \eta_{12})^2 - (\eta_{21} + \eta_{03})^2]\end{aligned} \quad (8)$$

ARTIFICIAL NEURAL NETWORK (ANN)

The data classifier is a two layer feed-forward ANN with back propagation training. This type of network provides a non-linear mapping from a set of input variables to a set of output variables [10]. Two layer networks are capable of classifying the input space into convex regions. The output of an arbitrary j^{th} hidden neuron is given by

$$a_j = \sum_{i=1}^{d} \omega_{ji} x_i \quad (9)$$

where j refers to the layer of the network containing the neuron, and i refers to the index of the input. A bias term can also be added in the form of a weight, denoted ω_{j0}, and is included in the summation notation by summing from $i = 0$ with input $x_0 = 1$. The value of a_j is then put through a non-linear activation function $g(a)$, where these functions need not be identical between subsequent layers.

The outputs from the first hidden layer are then applied to the output layer which operates in a similar fashion. The total output function of a general two layer network is

$$y_k = \tilde{g}\left(\sum_{j=0}^{M} \omega_{kj} g\left(\sum_{i=0}^{d} \omega_{ji} x_i \right) \right) \quad (10)$$

EXPERIMENTS AND RESULTS

Data was collected using an Anritsu 360A vector network analyzer (VNA) operating from 1 GHz to 12.4 GHz. The system uses a monostatic antenna configuration with a double-ridge horn antenna. The forward reflection S-parameter (S11) is utilized as the radar response for subsequent signal processing. The antenna is always directed with maximum power towards the ground. In our laboratory setup, the ground medium is dry silica sand with a dielectric constant of $\varepsilon_r \approx 2.4$.

Multiple target configurations were considered, including metallic targets and metallic and non-metallic clutter. Twenty eight different B-scans were gathered and processed. These B-scans varied in length from 40 cm to 150 cm, collected at 1cm intervals. Certain targets were considered valid 'landmine' targets, while others were considered to be targets that we wish to ignore. For the purposes of this preliminary study, we deemed metallic targets with a maximum dimension less than 5 cm as 'non-landmine' targets which we intended our automatic detector to ignore. Targets were buried at depths varying from 1 cm to 15 cm, with clutter placed in multiple configurations around the targets. Clutter was buried beside, around and above valid targets. Clutter consists of both metallic and dielectric objects.

Dielectric 'landmine' targets were considered, but were not reliably detectable using this automatic detection method. It seems that more information than simply magnitude and phase, such as the use of symmetry filters [11] and/or the use of polarization information to amplify the target signatures from symmetric targets, will have to be used. Thus, we also chose to ignore all non-metallic targets.

To apply the invariant moments to the collected data, one must first decide on the window size of the image $f(x, y)$ on which to apply the invariant moments. For example, the moments could be calculated for a long (1 meter) scan, or for a single A-scan. Since the final goal for this system is to process GPR data in real-time, calculating invariant moments on 1 meter scans is not a desirable solution. To this end, a sliding window is used starting at each A-scan. The windows chosen are 3, 5 and 10 A-scans wide (i.e. 3, 5 and 10 cm portions of the B-scans). These are individually processed using the invariant moment technique.

Of the 28 B-scans, 9 were selected as training data for the ANN. With apriori knowledge of the targets involved, the seven invariant moments were labelled (with a one or zero for target or non target) within each training B-scan. These same 9 scans were used to train all neural networks. A training scan, with corresponding moments can be seen in Figure 1.

Scale Invariance

The method used to test scale invariance is to change the zero-pad factor used in the IFFT processing of each A-scan. Changing the zero-pad factor simulates a change in the permittivity of the ground medium. It should be noted that this is not exactly the same as a differing ground type, because a different permittivity would create a different reflected wave from the same target. However, for the purposes of the metallic targets considered here, it is assumed that this change would be negligible.

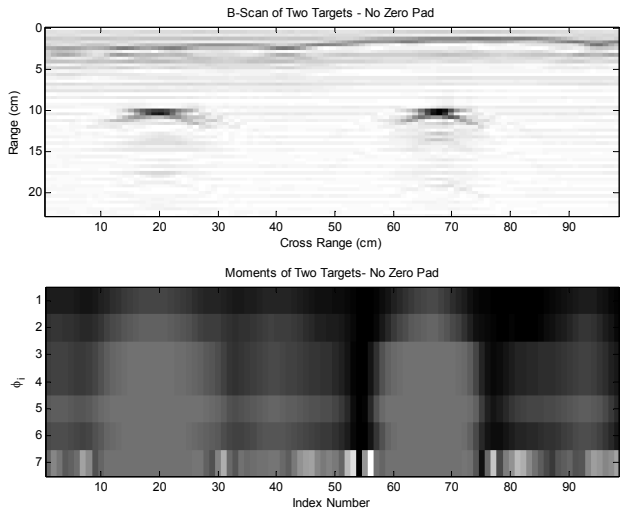

Figure 1. (Top) Non-Zero Padded B-scan of 2 targets (Bottom) Invariant Moments of B-scan

These results are shown in Figure 1 (no zero-padding) and Figure 2 (with 4 times zero-padding). As can be seen, there is negligible difference in the moments between the zero padded and non zero padded data. The differences that do occur are due to the fact that zero padding creates an interpolated image, rather than a strictly scaled image.

In order to provide a network capable of learning the required target distribution, while still being able to generalize new inputs, five neurons in the first hidden layer and a single neuron in the output layer are used.

The training process of the network is very sensitive to the random initial weight vector. The training algorithm attempts to minimize the mean square error, but may settle inside local minima inside the error space. There is no guarantee that the global error minimum will be found. To explore this variability in the network, the network, for each window size, was trained with the same data 5 different times (using 5 random initial weight vectors).

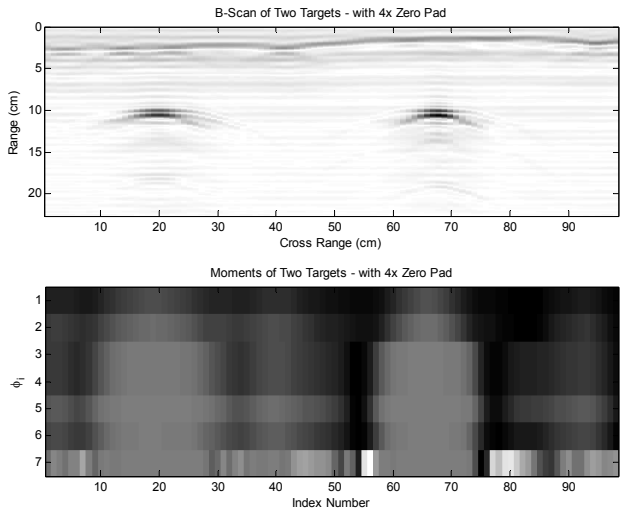

Figure 2. (Top) Zero Padded B-scan of 2 targets (Bottom) Invariant Moments of B-scan

Table 1: Window Size = 3 Cells - 21 Total Targets

Series	Found (%)	False Negatives (%)	False Positives (#)
1	81	19	7
2	95	5	9
3	95	5	6
4	90	10	6
5	95	5	6
Average	91.2	8.8	6.8

Table 2: Window Size = 10 Cells - 21 Total Targets

Series	Found (%)	False Negatives (%)	#False Positives
1	67	33	20
2	57	43	9
3	48	52	8
4	57	43	4
5	57	43	9
Average	57.2	42.8	10

In Tables 1 through 2, the percentages of targets found, false negatives (i.e., a missed target), and false positives are shown. False positives are defined as a positive output from the neural network when no target was present. An output of two accurate classifications with no false positive results is shown in Figure 3. An example of a false positive response can be seen in Figure 4.

Results show that this technique alone is not adequate as a target identifier. Far too many false negative indications and false positive indications are evident. However, there is a high percentage of accurate classifications across a large range of data. The small window size (window size of 3) provides the best results of this study. This occurs because the larger windows observe a larger portion of the total

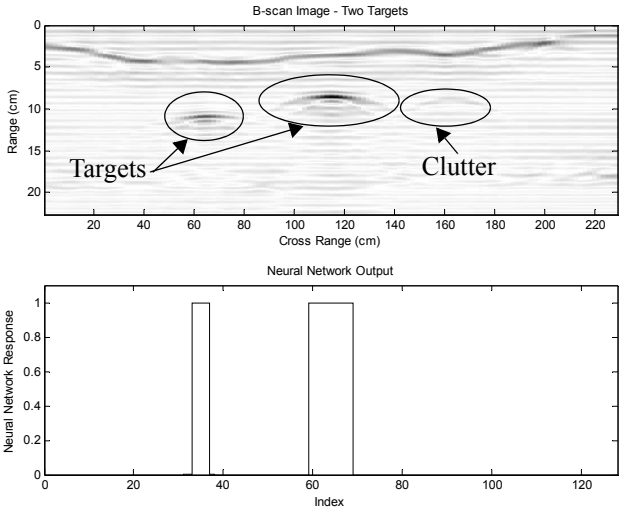

Figure 3. (Top) B-scan of two targets (Bottom) Output from ANN

image. When there is a target present, the target will affect the invariant moments less in the larger windows.

Table 3: Window Size = 5 Cells - 21 Total Targets

Series	Found (%)	False Negatives (%)	#False Positives
1	62	38	9
2	72	28	4
3	57	43	4
4	76	24	11
5	81	19	13
Average	69.6	30.4	8.2

A second neural network with fifteen neurons on the hidden layer was also examined. This network proved to identify a similar number of targets, but the number of false positive indications was approximately triple that of the five neuron network.

CONCLUSION

Preliminary investigation into the use of Hu's seven invariant moments as a feature extraction technique has been performed. The results of the moment based feature extraction were then applied to a neural network. Results indicate that while this technique has some advantages, it alone is not a sufficient method to detect targets. Many false negatives occur, even in a controlled laboratory test environment. The level of false positives is also fairly high in all three cases.

Future work will concentrate on incorporating more features that are suitable for use in indentifying targets. To achieve the ultimate goal of dielectric and metallic landmine detection, other pre-processing methods, such as observing target symmetry and polarization information, need to be employed.

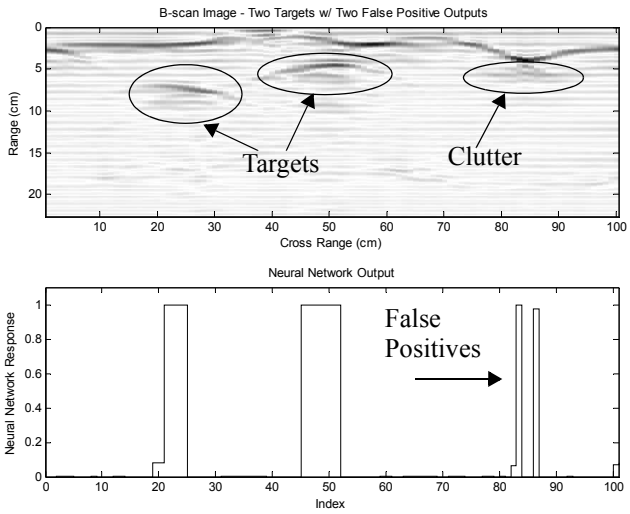

Figure 4. (Top) B-scan of two targets, (Bottom) ANN output with two false positive indications.

REFERENCES

[1] S. Perrin, A. Bibaut, E. Duflos, P. Vanheeghe, "Use of Wavelets for Ground-Penetrating Radar Signal Analysis and Multisensor Fusion in the Frame of Land Mine Detection" *IEEE Int. Conf. on Sys. Man and Cyb.*, Vol. 4, Oct. 8-11, 2000 pp. 2940 - 2945.

[2] B. Barkat, A. M. Zoubir, C. L. Brown, "Application of Time-Frequency Techniques for the Detection of Anti-Personnel Landmines," *Proc. of the Tenth IEEE Workshop on Stat. Sig. and Array Proc.*, Aug. 14-16, 2000, pp. 594 - 597.

[3] J. W. Brooks, M. W. Maier, "Application of System Identification and Neural Networks to Classification of Land Mines" *EUREL Int. Conf.: The Detection of Abandoned Land Mines: A Humanitarian Imperative Seeking a Technical Solution*, (Conf. Publ. No. 431), Oct. 7-9, 1996, pp. 46 - 50.

[4] J. Tkac, S. Spirko, L. Boka, "Radar Object Recognition by Wavelet Transform and Neural Network," *13th Int. Conf. on Microwaves, Radar and Wireless Comm.*, MIKON-2000. Vol. 1, May 22-24 2000, pp. 239 - 243.

[5] S. Shihab, W. Al-Nuaimy, Y. Huang, A. Eriksen, "A Comparison of Segmentation Techniques for Target Extraction in Ground Penetrating Radar Data," *Proc. of the 2nd Int. Workshop on Advanced GPR.*, May 14-16, 2003, pp. 95 - 100.

[6] M. P. Kolba, I. I. Jouny, "Clutter Suppression and Feature Extraction for Land Mine Detection using Ground Penetrating Radar," *IEEE Int. Symp. Ant. and Prop.*, Vol. 2, June 22-27, 2003, pp. 203 - 206.

[7] H. Brunzell, "Extraction of Discriminant Features from Impulse Radar Data for Classification of Buried Objects," *IGARSS '97, IEEE Int. Conf. on Remote Sensing*, Vol. 3, Aug. 3-8, 1997, pp.1285-1287.

[8] Hu-Ming-Kuei, "Visual Pattern Recognition by Moment Invariants," *IEEE Trans. on Information Theory*, Vol. 8, No. 2, Feb 1962, pp. 179-187.

[9] Rafael C. Gonzalez and Richard E. Woods, *Digital Image Processing*, 2nd Edition, Prentice Hall, 2002.

[10] C. M. Bishop, *Neural Networks for Pattern Recognition*, Oxford, 1995.

[11] Phelan, M. "A Group Theoretical Symmetry Filter For Improved Substance Imaging," *M.Sc. Thesis*, University of Manitoba, April 2004.